CONF-780461--1

MASTER

PREPRINT UCRL-80862

Lawrence Livermore Laboratory

THEORETICAL INTERPRETATION OF HIGH-Z DISCS IRRADIATED WITH 1.06 μ LASER LIGHT

M. D. Rosen, W. C. Mead, J. J. Thomson, and W. L. Kruer

March 31, 1978

Presented at the 8th Annual Conference on Anomalous Absorption of Electromagnetic Waves, Tucson, Arizona, April 19-21, 1978.

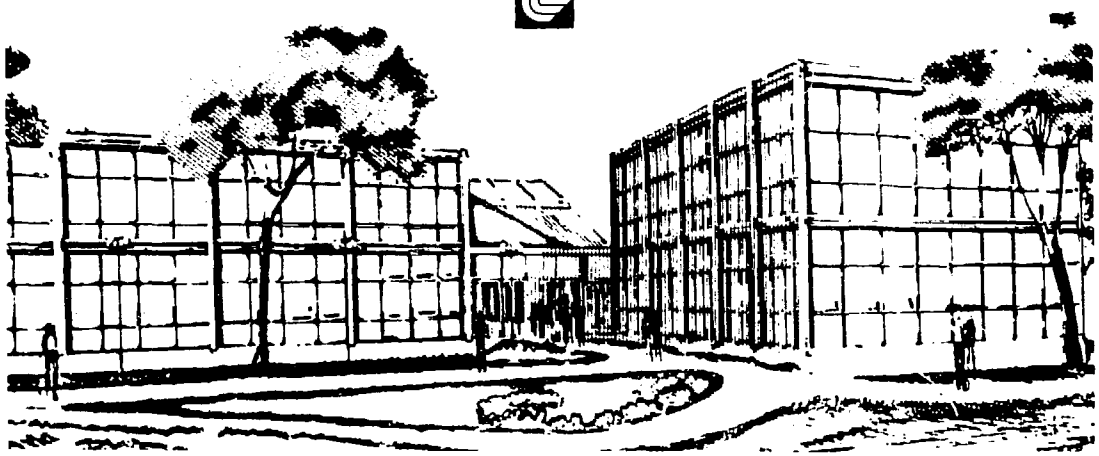

THEORETICAL INTERPRETATION OF HIGH-Z DISCS IRRADIATED WITH 1.06 μ LASER LIGHT*

M. D. Rosen, W. C. Mead, J. J. Thomson, and W. L. Kruer

University of California, Lawrence Livermore Laboratory
Livermore, California 94550

ABSTRACT

High Z discs have been irradiated with 1.06 μ laser light at intensities between 7×10^{13} and 3×10^{15} W/cm , and pulse lengths between 200 and 1000 ps. Due to the high Z, inverse bremsstrahlung becomes an important absorption effect and competes strongly with resonance absorption and stimulated scattering. We find that inhibited electron thermal conduction and non-LTE ionization physics are important. Their inclusion in the LASNEX modeling results in steepened temperature and density profiles near critical, thus producing a several keV underdense corona. These conditions bring what would otherwise be 100% inverse bremsstrahlung absorption down to the experimentally observed values (50% at 10^{14} W/cm). The non-LTE physics is essential to correctly compute the level populations of the high Z atoms moving rapidly through a steep density gradient into the corona. This modeling also shows that x-rays are emitted in a thin overdense region, and on a time scale 50% longer than the laser pulse. Both of these effects are seen in the experiments.

*Work performed under the auspices of the U.S. Department of Energy by the Lawrence Livermore Laboratory under contract No. W-7405-ENG-48.

High-Z discs have been irradiated[1] with the 1.06 μ light generated by the Argus laser system at Lawrence Livermore Laboratory. The light intensity has been varied from 7×10^{13} to 3×10^{15} W/cm^2 by changing laser energies from 100 to 500 J, laser pulse widths from 200 to 1000 ps, and irradiated spot diameters from 80 to 250 μ. Due to the high Z of the material, typically gold, inverse bremsstrahlung, the classical light absorption mechanism, becomes an important effect and competes strongly with resonance absorption and stimulated scattering. The details of the competition among these processes are quite subtle and the present experiments represent an extension of previously reported work[2,3] into longer pulse, higher intensity parameter regimes.

Figure 1 shows the experimental set-up. Direct measurement[4] of absorbed energy is performed using calorimeters that detect ions and x-rays but subtract out the scattered 1 μ light. The scattered light is measured with PIN diodes thus giving a purely optical measure of absorption. Finally, an enclosing calorimeter performs the same task as the PIN diodes, but covers the solid angle around the disc in a continuous fashion. Sub-keV 5 channel K-edge filtered x-ray detectors, with 300 to 500 ps time resolution, measure the low energy x-ray distribution, as do flat response sub keV calorimeters. These also give information on the angular distribution of these x-rays. Crystal spectrometers above 1 keV give information on characteristic line emission and on suprathermal electrons which produce hot x-ray tails in the spectra. An x-ray microscope gives spatially resolved emission regions, while an x-ray streak camera gives time resolved information.

In this paper we use the LASNEX[5] code to model the relevant physics of these experiments. The absorption model we use allows for inverse bremsstrahlung as a light ray refracts through the underdense plasma. In addition, 30% of whatever light that reaches the critical surface (some of which has been absorbed on the way in by inverse bremsstrahlung) is absorbed by collective effects such as resonance absorption. This 30% number is based on plasma simulations[6] and on absorption experiments on parylene discs.[7] The important physical effect of stimulated scattering is not included in the LASNEX modeling, though we will estimate its effect on the absorption later in this paper.

Figure 2 demonstrates the general energy balance of these experiments. The absorbed laser light heats electrons at the critical surface, and below. Electron thermal conduction then heats the overdense region, where the electron-ion coupling is strong. Energy is lost in ionizing the high-Z atoms and in heating the electrons and ions. In addition there are further losses due to radiation and convective energy of ion blowoff into the vacuum. When the simulations were first done, we typically found 99% absorption for the long pulse experiments. Figure 3 shows why this was plausible. The high-Z material cooled the electrons radiatively, increasing the collision frequency ($\nu_{ei} \sim ZT_e^{-3/2}$) and thus increasing the inverse bremsstrahlung absorption. However, despite this plausible argument, Figure 4 shows the experimental results, with typically 50% absorption! We have since found that inhibited electron thermal conduction, and non-LTE ionization physics are important effects to be included in the

modeling. Figure 5 shows why these two effects reduce the absorption to levels near those of the experiment. The inhibition reduces transport into the overdense region. Thus only a small amount of material is heated to several keV temperatures and forms a hot low density corona. This results in a sharp transition from cool overdense material, which has not been reached by the inhibited thermal front, to the hot corona. This reduces the absorption scale length. At critical, an electron-electron collision can take tens of picoseconds. An ion moving at the sound speed across this thin transition layer (a few microns thick) takes only a few picoseconds. In addition, radiative recombination takes place on a similar, short time scale. Thus non-LTE ionization physics must be used instead of the usual Saha equilibrium model. The non-LTE physics tends to lower the $\bar{Z}$ and thus further reduces the absorption down to experimental levels.

Figure 6 shows a leading candidate for inhibited conduction: the two-stream[8] instability. The cold return current neutralizing the hot electron current gives rise to a shifted Maxwellian distribution centered around a drift velocity, V_d. Once V_d becomes greater than c_s, the positive slope at c_s causes electron Landau growth leading to ion turbulence and the enhanced collisionality and transport inhibition associated with it. This assumes that $c_s \gg V_i$ so that there is no ion Landau damping to counter the instability. The simplest nonlinear model is to assume that the resulting ion turbulence causes V_d to hover near the point of onset of significant growth; i.e. $V_d \approx c_s$. Thus the inhibition is roughly $c_s/V_e \approx 0.01$. The condition

$c_s \gg V_i$ is equivalent to $ZT_e \gg T_i$ which is achieved in much of parameter space in high-Z plasmas. However theoretical uncertainties in growth rate and saturation level lead to some questions about the actual level of transport inhibition produced. Other possible mechanisms are macroscopic and microscopic magnetic fields.

Figure 7 contrasts n_e and T_e profiles for an inhibited vs. non-inhibited run. Note the steepened profile and hot corona of the inhibited modeling. The non-inhibited run's X_c moves further out than the inhibited one, since enhanced thermal transport inward blows more bulk plasma outward. Figure 8 shows how the absorption and emission profiles differ in the two cases. Note the much wider emission region for the non-inhibited case. This implies too much energy lost through radiation, whereas the experimental levels are much closer to those implied by the thinner emission region of the inhibited case.

Figure 9a compares the LASNEX absorption results (both inhibited and non-inhibited modeling) vs. experiments, and clearly shows the importance of including the inhibition. Nonetheless, there still seem to be discrepancies even in the inhibited case. Theoretical estimates of stimulated Brillouin scattering can be obtained by interfacing the models[9] and simulations[10] with the density and temperature profiles from LASNEX runs. The estimates for the 3×10^{15} W/cm^2 shots predict that $\approx 50\%$ of the laser energy can be lost, never to reach the critical surface. In support of the estimates is the strong experimental evidence that such processes are indeed occurring. A red shift in the backscattered light is observed, a clear indication of

Brillouin backscatter. These 50% loss figures are approximately what is needed to bring the LASNEX absorption numbers into agreement with the experiments for the high intensity cases (40% becomes 20% and 60% becomes 30%). For lower intensities (3×10^{14} W/cm^2), 15% loss due to stimulated scattering is predicted, reducing the 70% absorption figure to 60%, in close agreement with the 50% experimental number. These corrections are summarized in Figure 9b.

There is additional evidence that the model is correctly simulating the experiment. Figures 10a, 11a show x-ray microscope pictures of a 2 keV emission region for low and high intensity runs compared with LASNEX simulations. Figures 10b, 11b compare the non-inhibited vs. the inhibited model with the obvious conclusion that only the inhibited model can match the experiment. Figures 12 and 13 show the time behavior of the 400 eV x-rays for the two models. Once again agreement with experiment is closer using the inhibited model. Figures 14 and 15 show the close agreement of the predicted spectra with the experimentally observed one as long as the inhibited model is used. Figure 16 shows that for high intensity shots one must reduce the resonance absorption fraction from 30% to 7% in order to reproduce the hot x-ray tail. This is a reflection of stimulated scattering processes at work, denying the light access to the critical surface where resonant absorption occurs.

Figure 17 shows the difficulty that LTE physics encounters when attempting to reproduce the experimentally observed spectra that non-LTE matched so successfully. LTE's over-estimation of the ionization

(its neglect of photo recombinative processes) results in the super-enhancement of high energy spectral lines and thus fails to match the experimentally observed spectrum.

A simple model can predict the LASNEX scaling of absorption, and thus, by implication, the experimental values, when stimulated scattering is properly taken into account. The energy per unit area I_T heats matter into a depth λ to a temperature T (Figure 18). For λ we take $V_{th} \nu_{ei}^{-1} \sim T^2$. Thus $I_T \sim n_{cr} T^2 T$ or $T \sim (I_T)^{1/3}$. The absorption fraction $f \sim T^{-3/2} k_{oL} \sim T^{-3/2}(T^{1/2}{}_T)$. Thus $f \sim {}_T{}^{2/3} I^{-1/3}$. Recalling that LASNEX allows for 30% of what remains after inverse bremsstrahlung to be absorbed, we obtain $f_{abs} = 1 - .7 \exp(-f)$. Figure 19 shows the simple model scaling prediction matching those of the complex LASNEX code. The model is normalized to the 3×10^{14} W/cm^2 case.

In conclusion, inhibited electron thermal conduction and non-LTE ionization physics are important effects to consider when modeling the interaction of 1.06μ laser light with high-Z materials.

ACKNOWLEDGMENTS

We wish to thank the many members of the Target Design Group, Code Development Group, Plasma Theory Group, Laser Plasma Interaction Group, and Diagnostics Development Group who contributed to this effort.

REFERENCES

1. M. J. Boyle, E. M. Campbell, L. Koppel, H. N. Kornblum, P. Lee, D. Phillion, R. Price, V. Rupert, W. Slivinsky, and G. Tirsell, "Characteristics of High Z Discs Irradiated with Nanosecond 1.06 μm Laser Pulses." Presented at this Conference.
2. R. A. Haas et al., Phys. Rev. Lett. 39, 1533 (1977).
3. P. J. Mallozzi et al., Fundamental and Applied Laser Physics (John Wiley and Sons, New York, 1973), p. 165.
4. H. G. Ahlstrom, UCRL-79819 (1977).
5. G. B. Zimmerman, UCRL-74811 (1973).
6. K. Estabrook et al., Phys. Fluids 18, 1151 (1975).
7. K. R. Manes et al., Phys. Rev. Lett. 39, 281 (1977).
8. B. Fried and R. Gould, Phys. Fluids 4, 139 (1961); R. C. Malone et al., Phys. Rev. Lett. 34, 7211 (1975); 13, 457 (1973).
9. D. W. Phillion et al., Phys. Rev. Lett. 39, 1529 (1977).
10. Kent Estabrook (private communication).

ABSORPTION AND SCATTERED LIGHT MEASUREMENTS

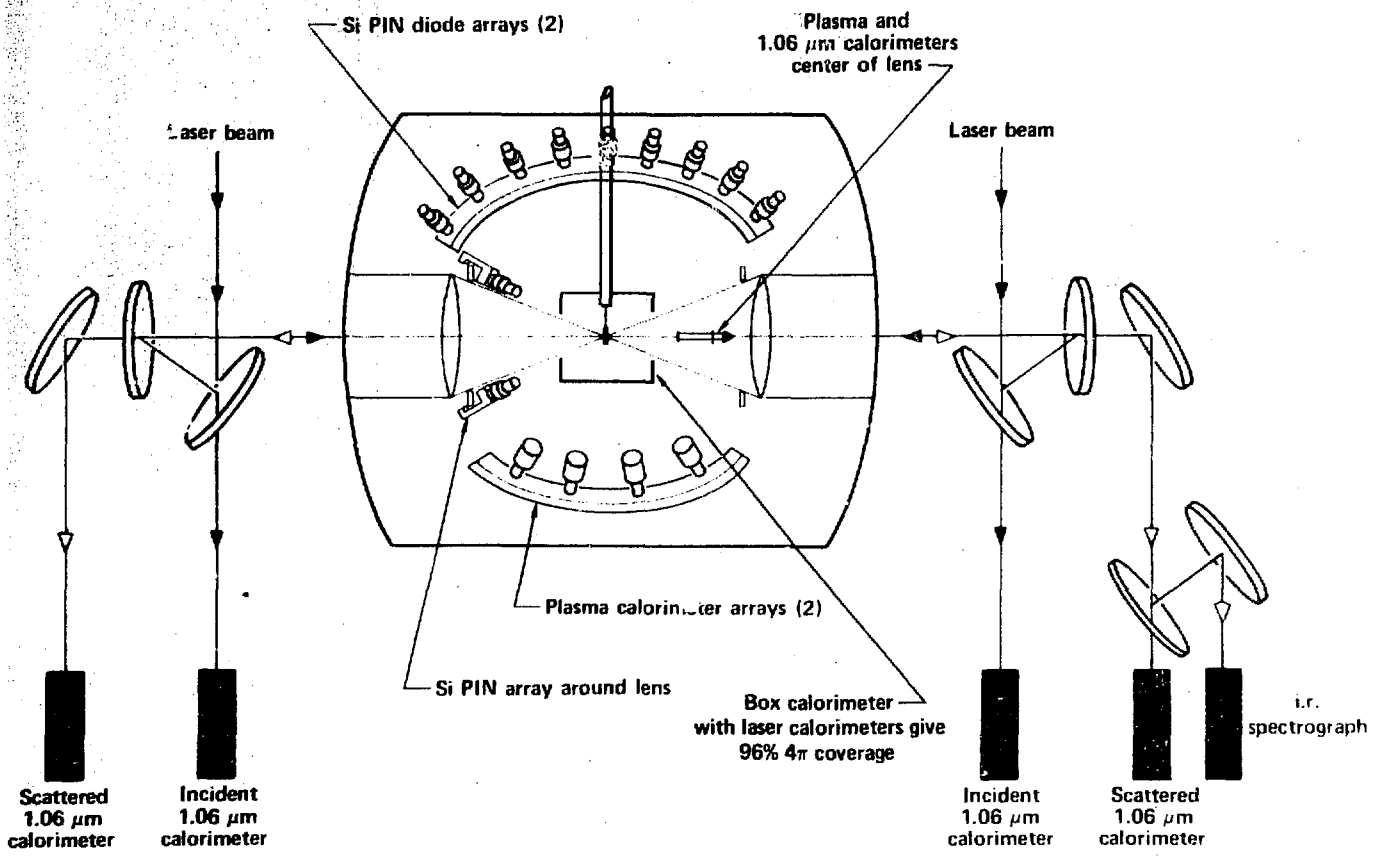

20-90-0378-1126

Figure 1

ENERGY BALANCE

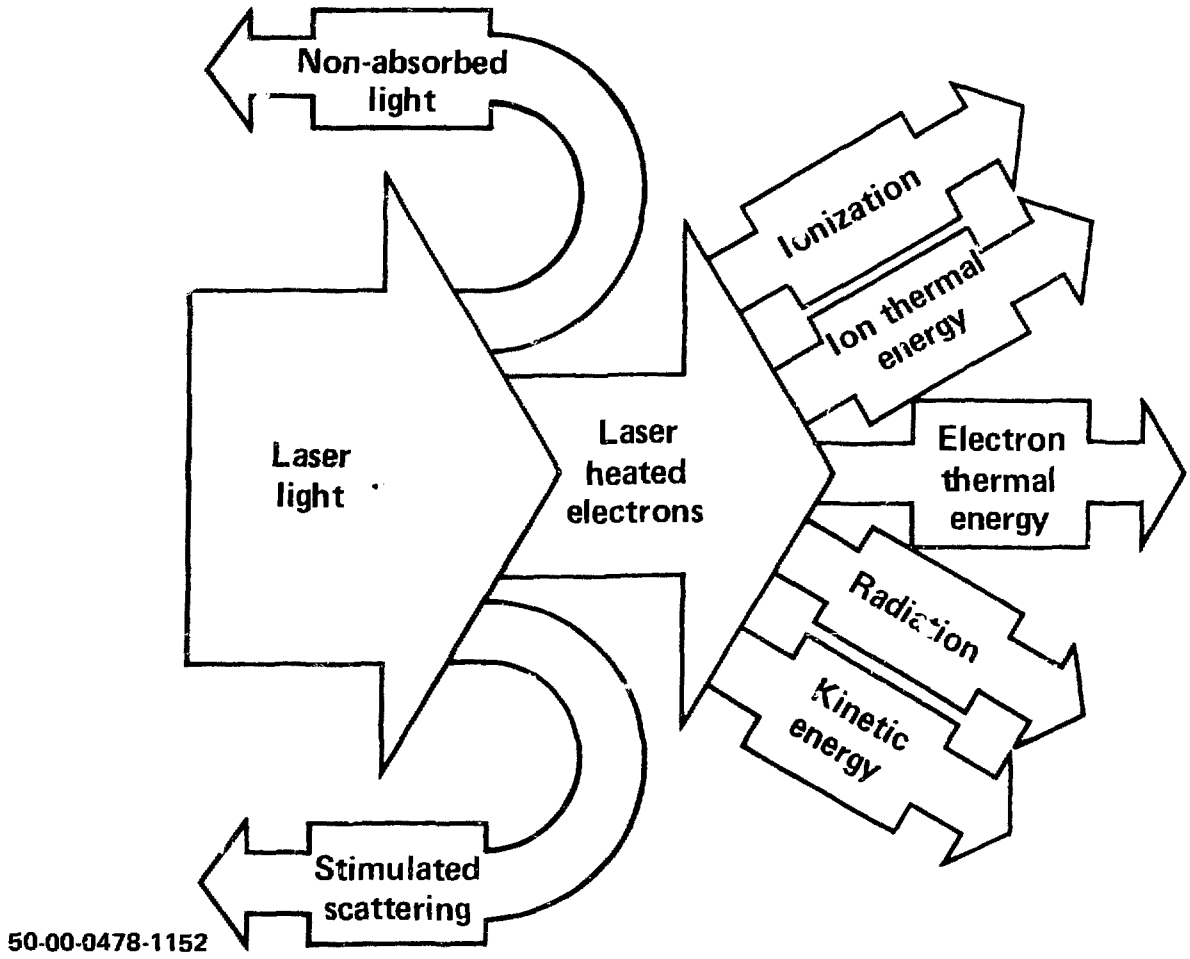

Figure 2

INVERSE BREMSSTRAHLUNG SEEMS TO LEAD TO 99% ABSORPTION

$$\frac{d}{dt}\left(\frac{\text{Energy}}{\text{Vol.}}\right) \sim \nu_{ei}\, n\, m_e V_{osc}^2 \sim (Zn^2 T^{-3/2})\, I$$

with density gradients there is also a $k_o L$ term

A) HI Z $\Rightarrow$ Radiative cooling of electrons
Cool, fairly dense absorption region

B) Long pulse $\Rightarrow$ Large $k_o L$

A) + B) $\Rightarrow$ 99% absorption

50-00-0478-1154

Figure 3

YET EXPERIMENTAL ABSORPTIONS ARE MUCH LOWER !

E(Joules) / τ (ps)	I (W/cm^2)	% ABS
300/200	$3 \cdot 10^{15}$	20
500/1000	$3 \cdot 10^{15}$	36
500/1000	$3 \cdot 10^{14}$	50
100/1000	$7 \cdot 10^{13}$	(>50)

50-00-0478-1164

Figure 4

TWO PHYSICAL EFFECTS CAN EXPLAIN THE DISCREPANCY BETWEEN NAIVE THEORY AND EXPERIMENT

A) Inhibited transport:

- Raises T_e
- Steepens profile (lowers koL and n^2)

B) Non-LTE treatment

- More realistic treatment of the hot corona that develops due to A)
- Lowers Z

A) + B) $\Rightarrow$ 70% absorption

TWO STREAM INSTABILITY: A HEAT FLUX INHIBITOR

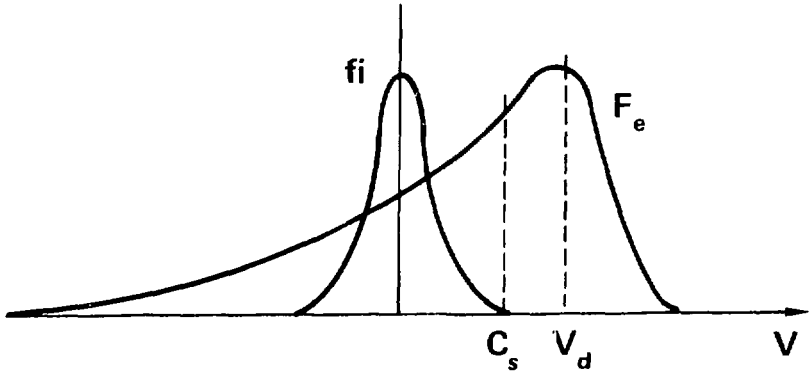

$$C_s \gg V_{th_i}$$

$$\| \qquad \|$$

$$\left(\frac{Z\,T_e}{Mi}\right)^{1/2} \gg \left(\frac{Ti}{Mi}\right)^{1/2}$$

$$J \sim \int f_e\, v dv = 0$$

$$Q \sim \int f_e\, v^3 dv \neq 0$$

Assume turbulence restricts

$$(V_d)_{max} \approx C_s$$

$$\Rightarrow Q_{max} \approx nm\, V_e^2\, C_s$$

$$\Rightarrow f \approx \frac{C_s}{V_e} \approx \sqrt{\frac{Z}{A}\,\frac{Me}{Mp}} \approx 0.01$$

50-00-0478-1163

Figure 6

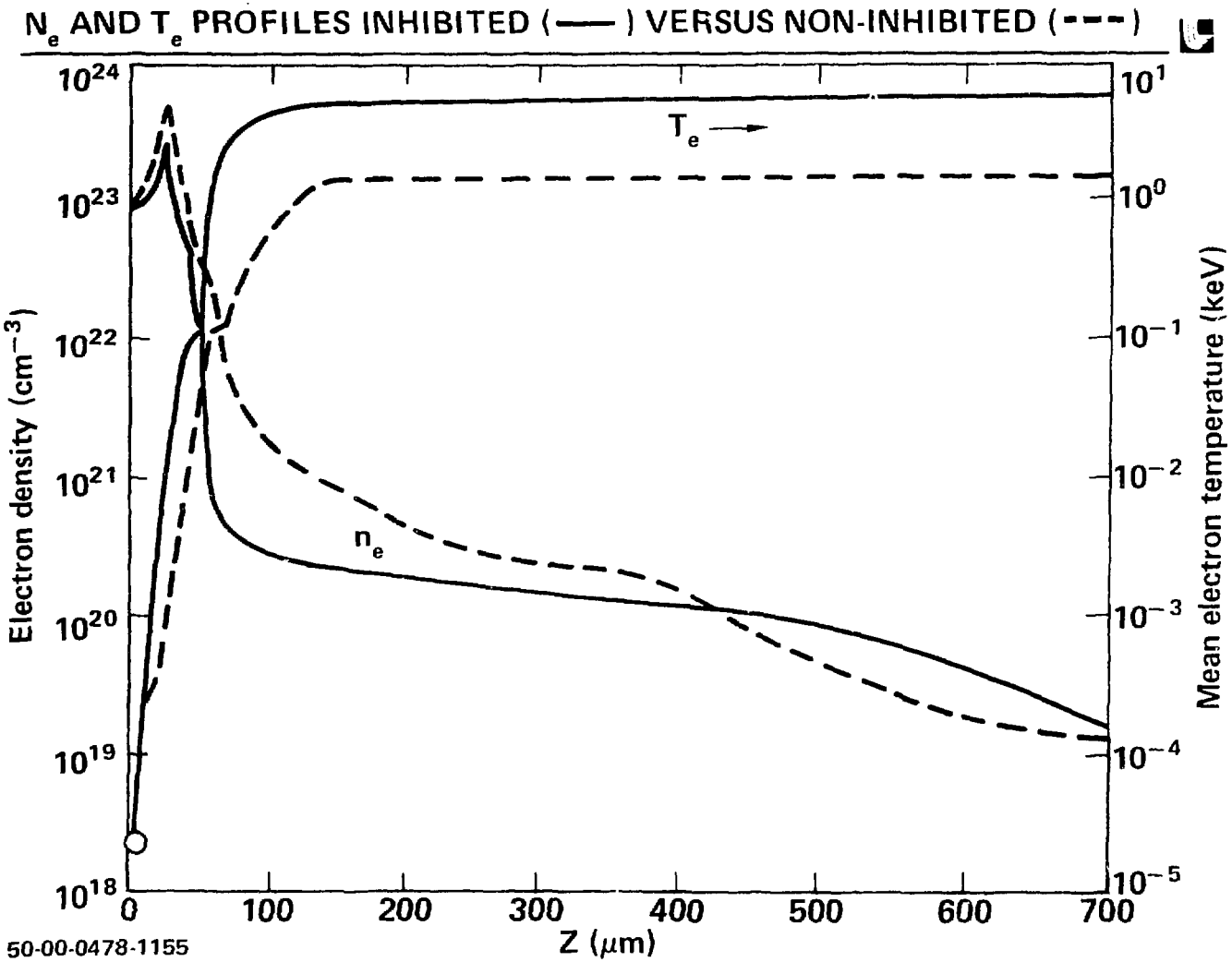
N_e AND T_e PROFILES INHIBITED (——) VERSUS NON-INHIBITED (- - -)
10^{24}
10^{23}
10^{22}
10^{21}
10^{20}
10^{19}
10^{18}
Electron density (cm^{-3})
10^{1}
10^{0}
10^{-1}
10^{-2}
10^{-3}
10^{-4}
10^{-5}
Mean electron temperature (keV)
T_e
n_e
0
100
200
300
400
500
600
700
Z (μm)
50-00-0478-1155

Figure 7

ABSORPTION AND EMISSION PROFILES INHIBITED (——) VERSUS NON-INHIBITED (– – –)

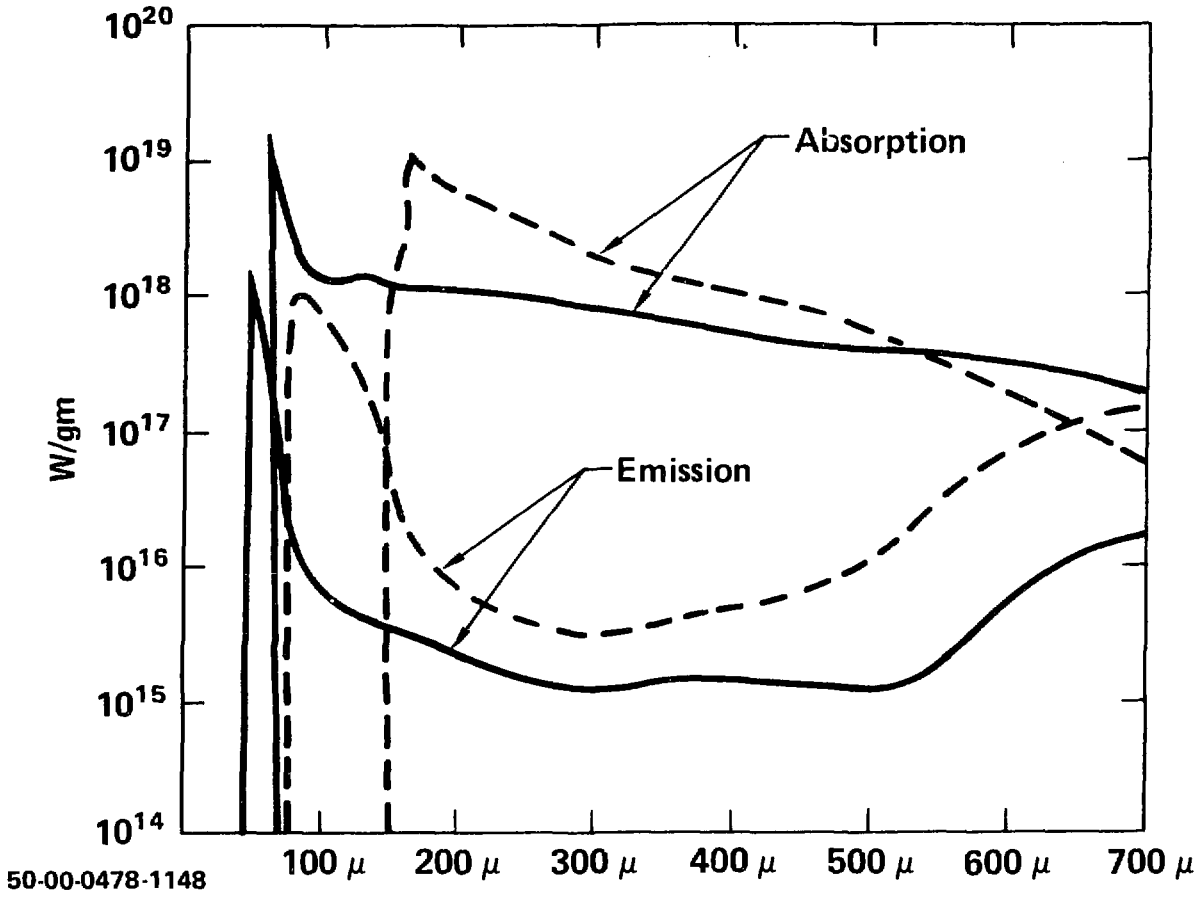

Figure 8

NON-INHIBITED AND INHIBITED LASNEX VERSUS EXPERIMENT

$E(J)/\tau(ps)$	$I\ (W/cm^2)$	% ABS NIL	% ABS IL	% ABS EXP
300/200	$3 \cdot 10^{15}$	60	40	20
500/1000	$3 \cdot 10^{15}$	90	60	36
500/1000	$3 \cdot 10^{14}$	99	70	50
100/1000	$7 \cdot 10^{13}$	99	80	(>50)

50-00-0478-1156

Figure 9a

CORRECTING FOR STIMULATED SCATTERING BRINGS THE CALCULATIONS CLOSER TO EXPERIMENT

E(J)/τ(ps)	I (W/cm^2)	% ABS $(1 - F_{ss}) \times LX$	EXP
300/200	$3 \cdot 10^{15}$	(0.5) × 40 = 20	20
500/1000	$3 \cdot 10^{15}$	(0.5) × 60 = 30	36
500/1000	$3 \cdot 10^{14}$	(0.85) × 70 = 60	50
100/1000	$7 \cdot 10^{13}$	(0.95) × 80 = 75	(>50)

50-00-0478-1151

Figure 9b

EXPERIMENT VERSUS LASNEX

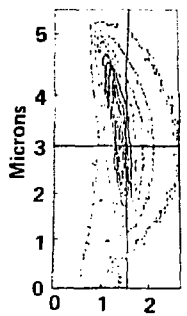

$\frac{100\ J}{1000\ ps}$; $8 \times 10^{13}\ W/cm^2$

X-ray microscope looking edge-on at 2 keV

TDG simulation of x-ray μscope

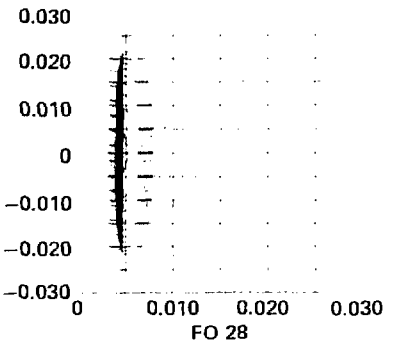

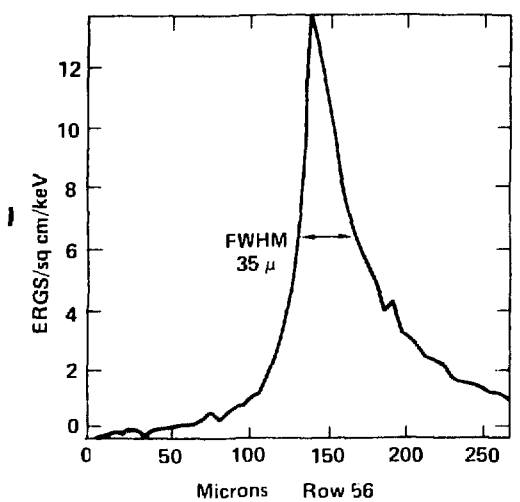

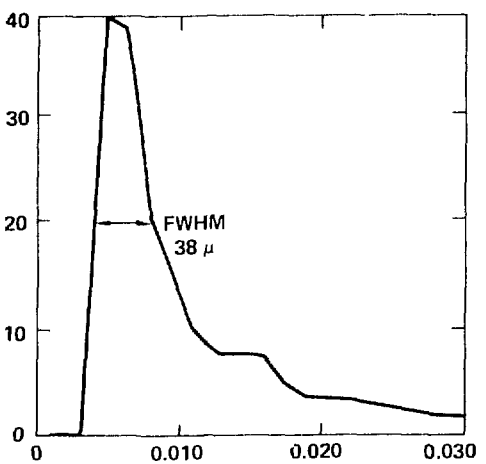

50-00-0478-1165

Figure 10a

(NON-INHIBITED) LASNEX VERSUS LASNEX (INHIBITED)

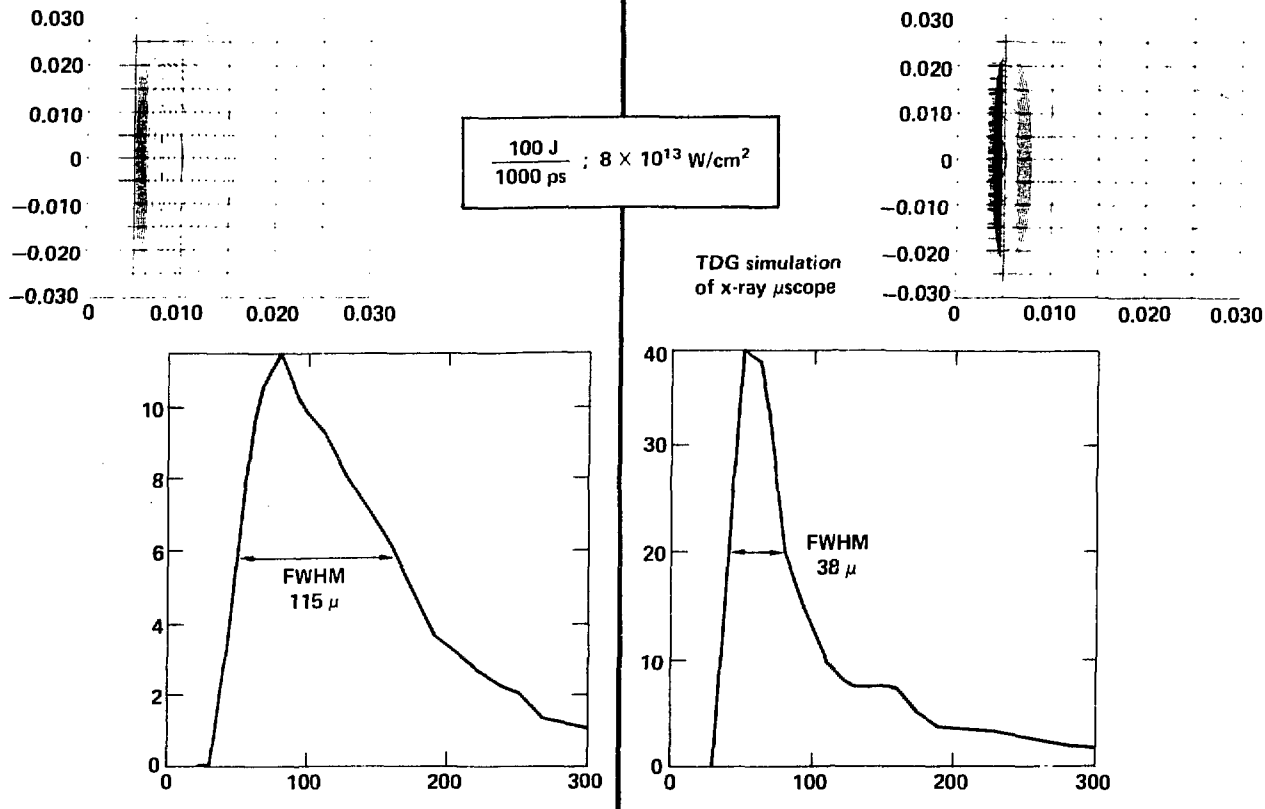

50-00-0478-1166

Figure 10b

EXPERIMENT VERSUS LASNEX

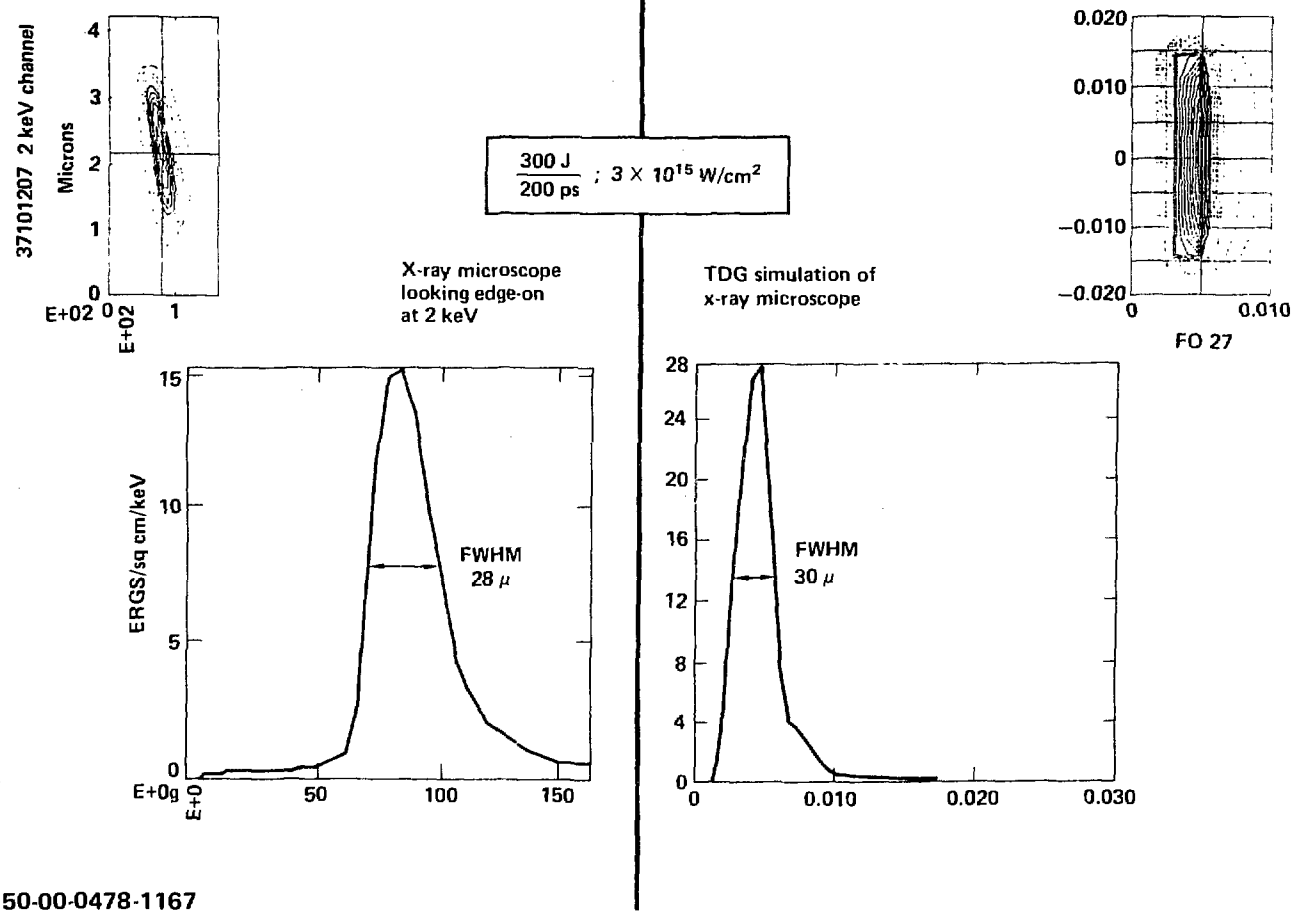

50-00-0478-1167

Figure 11a

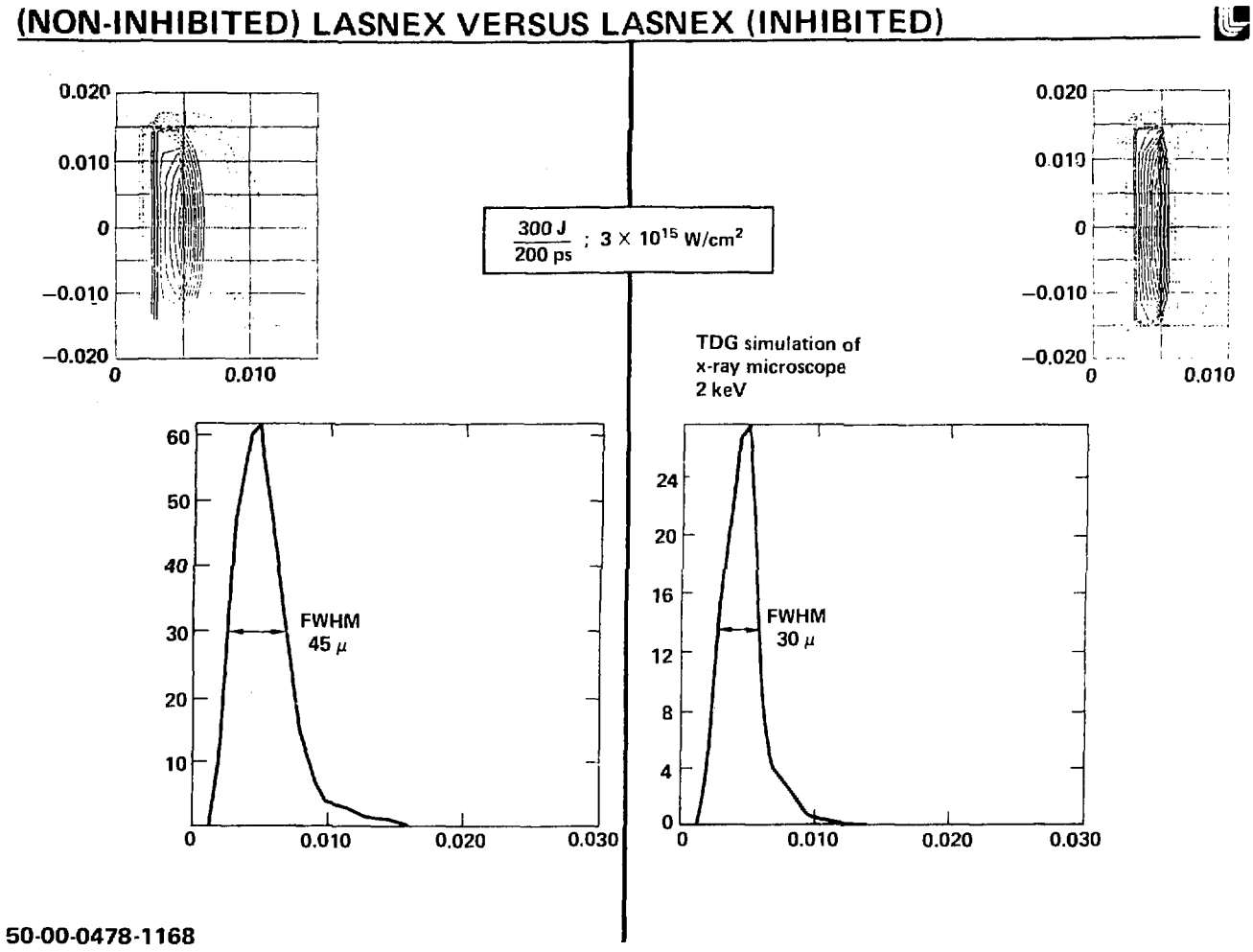
(NON-INHIBITED) LASNEX VERSUS LASNEX (INHIBITED)
0.020
0.010
0
−0.010
−0.020
0
0.010
300 J / 200 ps ; 3 × 10^15 W/cm^2
TDG simulation of
x-ray microscope
2 keV
0.020
0.010
0
−0.010
−0.020
0
0.010
60
50
40
30
20
10
FWHM
45 μ
0
0.010
0.020
0.030
24
20
16
12
8
4
0
FWHM
30 μ
0
0.010
0.020
0.030
50-00-0478-1168

Figure 11b

400 eV TIME RESPONSE: INHIBITED LASNEX

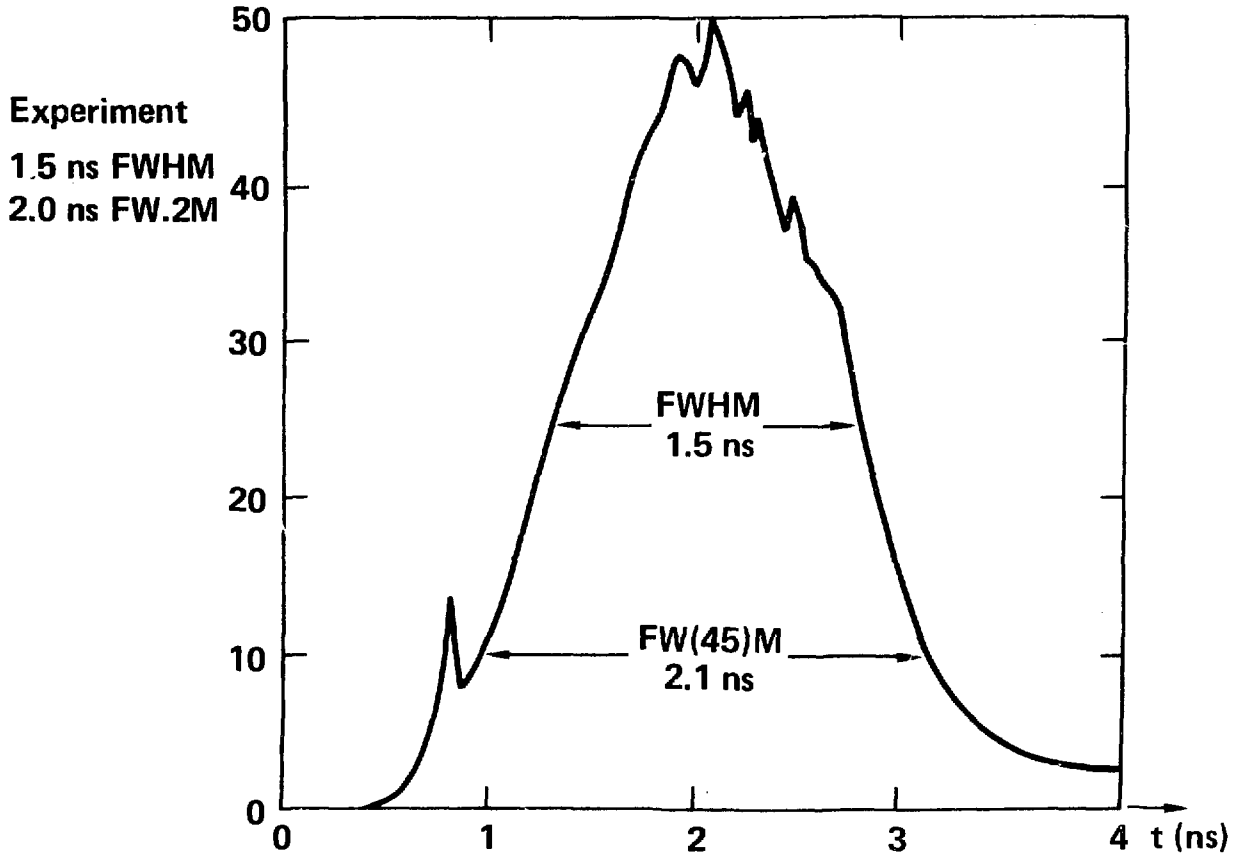

50-00-0478-1147

Figure 12

400 eV TIME RESPONSE: NON-INHIBITED LASNEX

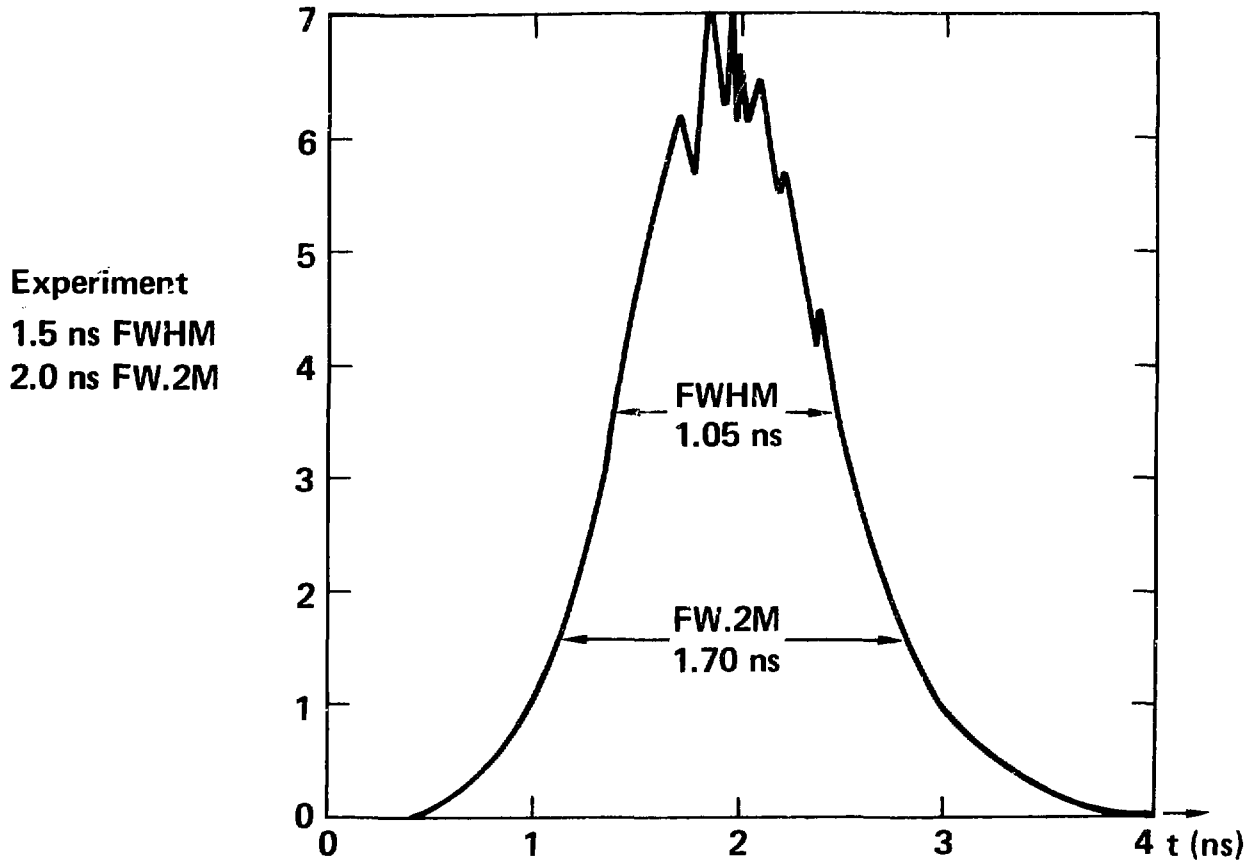

50-90-0478-1146

Figure 13

INHIBITED LASNEX MODEL MATCHES EXPERIMENTAL SPECTRUM

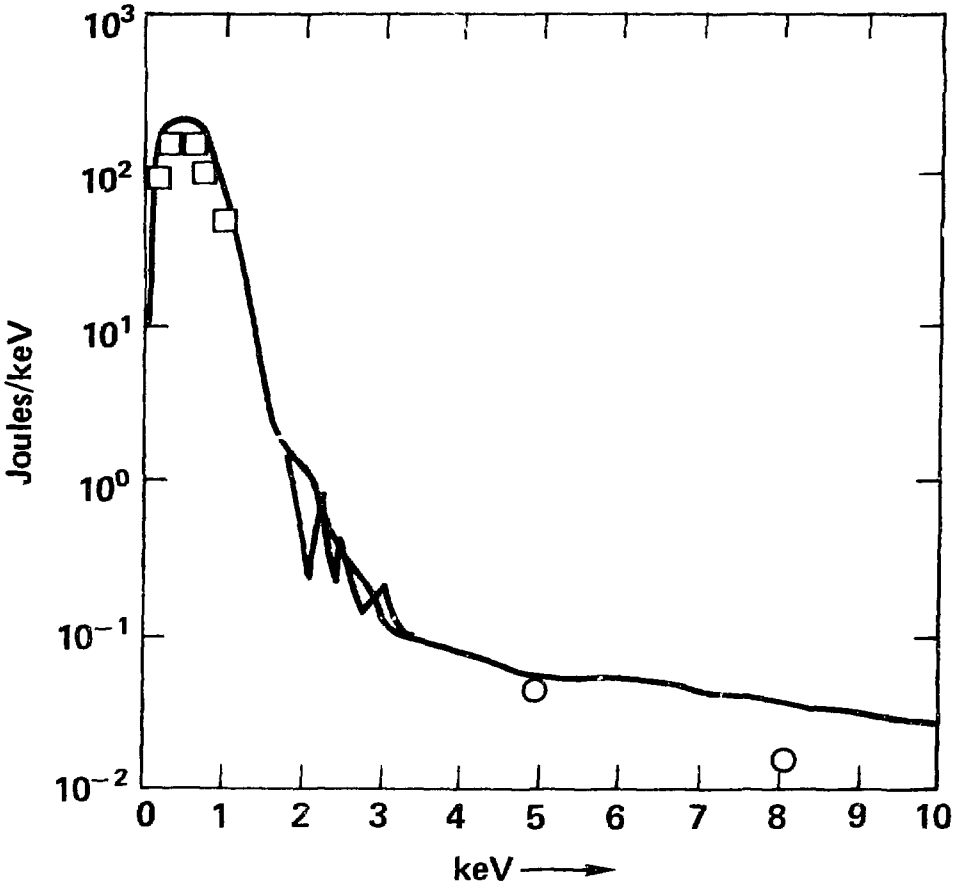

50-00-0478-1157

Figure 14

NON-INHIBITED LASNEX MODEL DOES NOT MATCH EXPERIMENTAL SPECTRUM

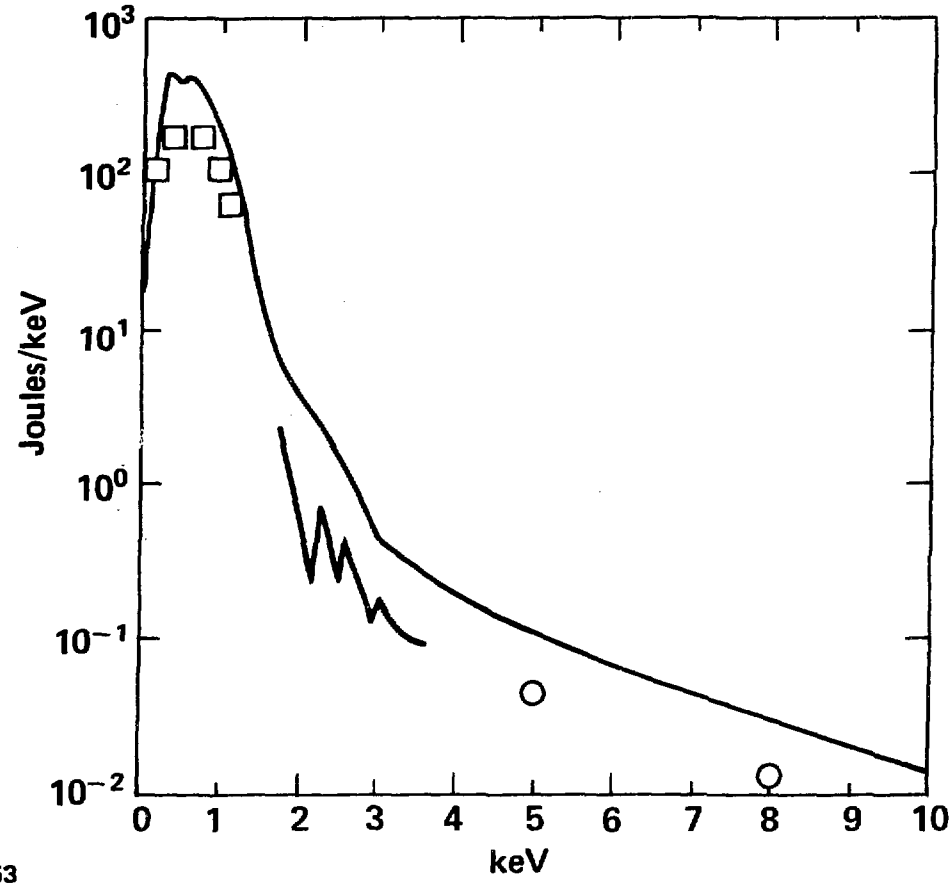

50-00-0478-1153

Figure 15

AT HIGH INTENSITIES EXPERIMENTS IMPLY REDUCED RESONANCE ABSORPTION

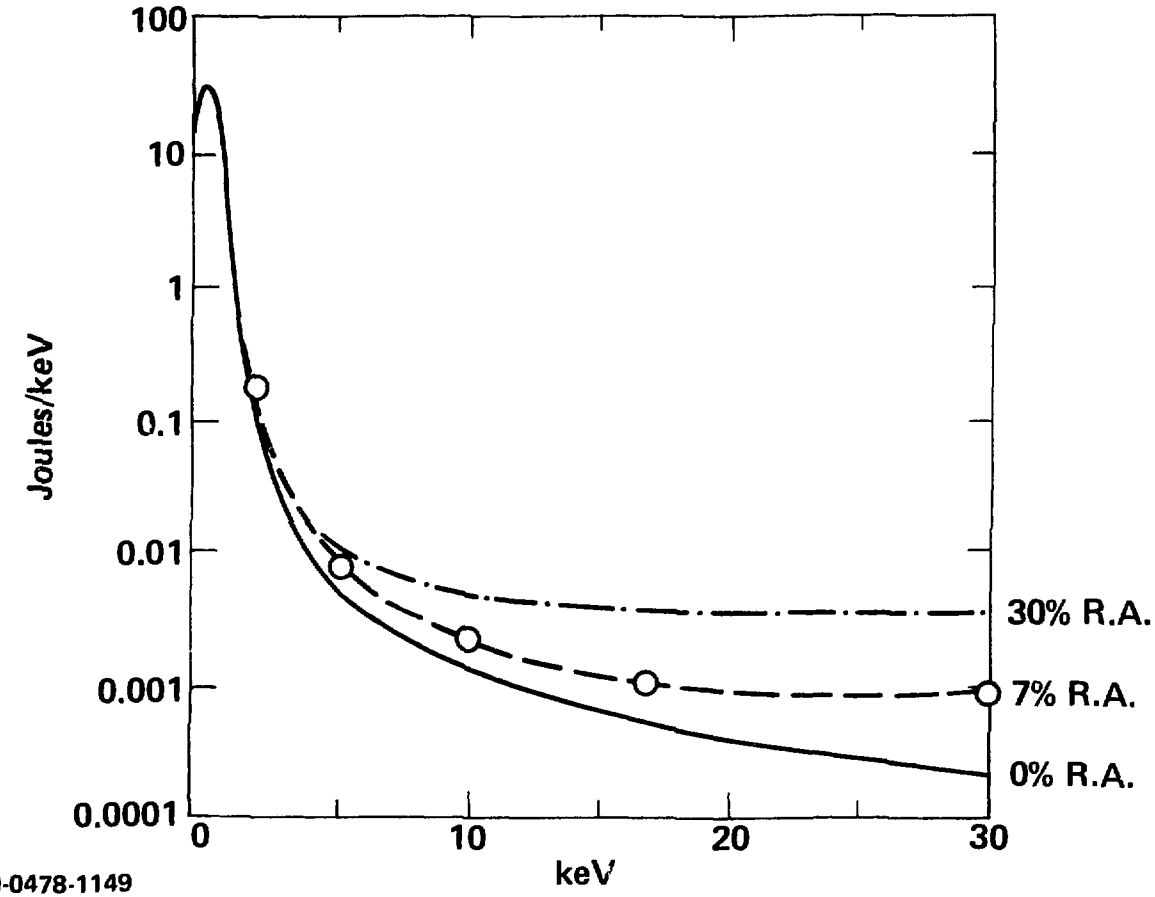

Figure 16

LTE MODELLING DOES NOT MATCH EXPERIMENTAL SPECTRUM

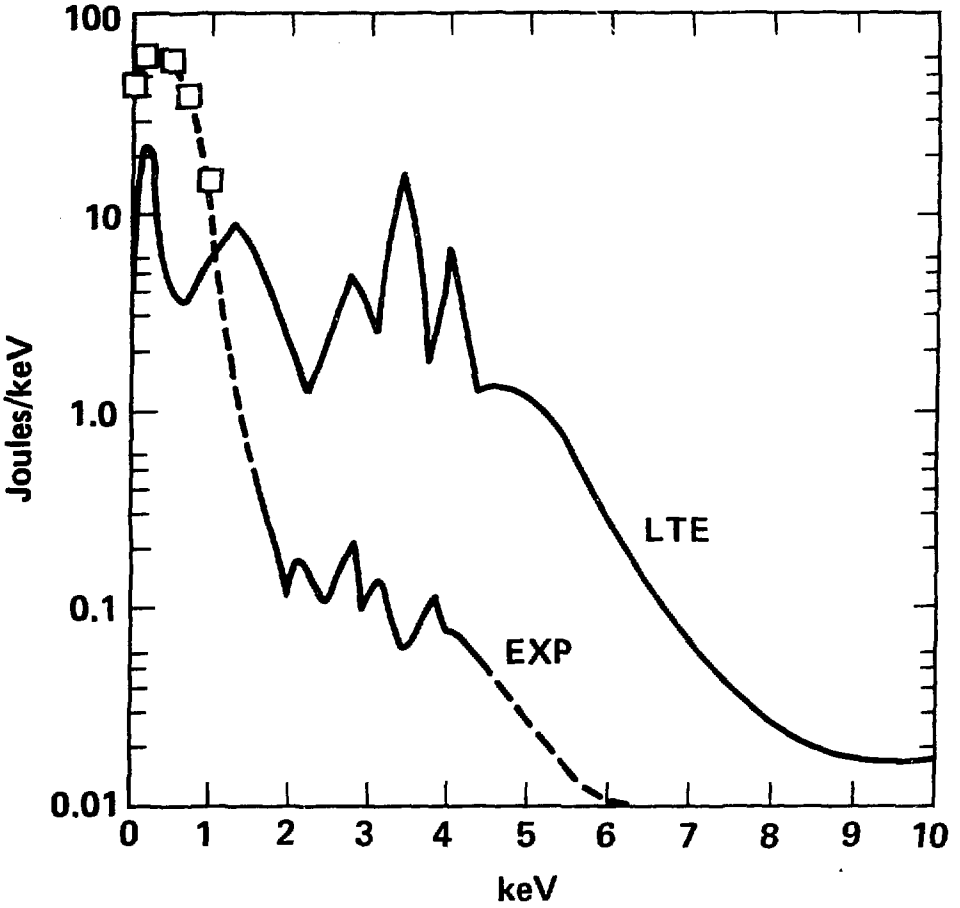

50-00-0478-1158

Figure 17

SIMPLE MODEL SCALINGS

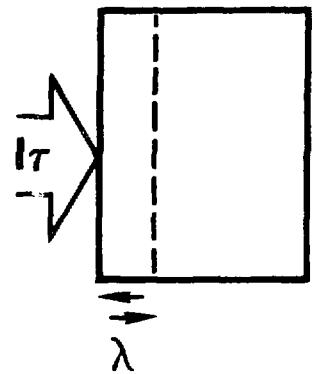

$$I\tau \ \frac{\text{Energy}}{\text{Area}} \approx n_{cr} \ \lambda \ T$$

$$\lambda \approx V_e \ \nu_{ei}^{-1} \sim T^2$$

$$\boxed{T \sim (I\tau)^{1/3}}$$

$$f_{I.B.} \sim T^{-3/2} \ L \sim T^{-3/2} \ (T^{1/2} \tau) \sim \tau^{2/3} \ I^{-1/3}$$

$$f_{abs} \approx (1 - \exp(-f_{I.B.})) + 0.3 \exp(-f_{I.B.}) = 0.7 \exp(-f_{I.B.})$$

50-00-0478-1159

Figure 18

SIMPLE MODEL SCALINGS MATCH THOSE OF LASNEX

		f_{abs} (%)		T_e (keV)	
τ (ps)	I (W/cm^2)	Model	Lasnex	Model	Lasnex
200	$3 \cdot 10^{15}$	39	40	8.0	7.6
1000	$3 \cdot 10^{15}$	56	60	12.3	12.9
1000	$3 \cdot 10^{14}$ *	70	70	6.0	6.0
1000	$7 \cdot 10^{13}$	82	80	4.1	3.5

*Normalization point

50-00-0478-1160

Figure 19